A 15 Meter Laser-Stabilized Imaging Interferometer

R. Stebbins, P. Bender

JILA, University of Colorado
Boulder, CO 80309-0440

C. Chen, N. Page, D. Meier

Jet Propulsion Laboratory, California Institute of Technology
4800 Oak Grove Drive
Pasadena, CA 91109

A. Dupree

Smithsonian Astrophysical Observatory
60 Garden St.
Cambridge, MA 02138

ABSTRACT

The LA.ser-Stabilized Imaging Interferometer (LAW concept is being developed as a candidate for the next generation of optical resolution beyond Hubble Space Telescope (HST). The essential ingredients are: a rigid and stable structure to minimize mechanical and thermal distortion, active control of the optical geometry by a laser metrology system, a self-deploying structure fitting into a single launch vehicle, and ultraviolet operation. We have modified earlier design concepts to fit the scale of an intermediate sized NASA mission.

Our present design calls for 240.5 m apertures arranged in a Milk Cross configuration and supported on four trusses (0.8 wide and 7.5 meters long). A fifth truss of similar dimensions, perpendicular to the primary surface, would function as a mast to support the secondary mirror and the laser metrology control points. Either separate interferometers or two guide telescopes would track guide stars. This instrument would have about 6 times the resolution of HST in the visible and. the same collecting area. The resolution would reach 2.5 mas at 150 nm.

The structure could be light, but sufficiently rigid to reduce the distortions caused by on-board disturbances to low levels. Materials such as carbon-carbon would be used to decrease thermal drifts, so that only low frequency control loops would be needed. The interferometer arms would fold along the mast for launch, and then automatically unfold and lock into place on orbit. Possible orbits are sun-synchronous at 900 km altitude, high earth orbit or solar orbit. Infrared capability could be included, if desired.

Keywords: imaging interferometer, space telescope, laser metrology

1. Introduction

1.1 Mission Concept

Our advancing knowledge of the Universe is constantly demanding higher-resolution images. The past decade has seen resolution advances in space-based telescopes, in adaptive optics systems on the ground, particularly in the IR, and in ground-based interferometers for astrometry. By the time that LASII is likely to fly, one might expect imaging interferometers operating in the IR on the ground, with laser guide stars for phasing each aperture. Such instrument will always have to combat three challenges: the manifold complexities of imaging

interferometry with many apertures subjected to terrestrial disturbances (e.g. vibration, air density fluctuations, pointing in a 1 g environment), the amplitude and bandwidth of the wavefront noise caused by atmospheric turbulence, and the transmission of the atmosphere. There are strategies for dealing with all but the last of these problems, but the problem of co-phasing all of the apertures makes for a steeply accelerating technical burden as the wavelength approaches the visible.

A spaceborne instrument is free of the turbulence and transmission problems, and the effect of disturbances can be reduced so that the active control systems need only have very modest bandwidth and dynamic range. The net result is that space telescopes can generally see to much fainter magnitudes and to much shorter wavelengths. Our goal is to provide six times the resolving power of HST in an Intermediate class mission. To this end, we have developed a concept for a spaceborne telescope having a 3% filled primary composed of actively positioned sub-apertures. The optics are mounted on a stiff, stable, lightweight structure, and every effort is made to reduce disturbances.

1.2 Related Work

Missions of this type were examined in a JPL study[2,3] directed by S. P. Synnott, which started in 1987. The study explored different approaches to imaging interferometry in space in enough detail to identify the areas of technology development where substantial work was needed for future mission studies.

In order to be specific, the results of the study were focused on a particular interferometer design concept, called the Filled-Arm Fizeau Telescope (FFT). The FFT had a diameter of 25-30 m and a Mills Cross geometry. Light from the very fast, partially filled primary was reflected from a secondary and additional mirrors to give an image with a long effective focal length. In this design, the possibilities of avoiding the use of a laser metrology system to maintain the instrument alignment and of pointing the telescope using an off-axis guide star observed through the same main optics were investigated.

Independently, a very brief study[4] looked at possible approaches which made use of laser stabilization of the optical system and guiding through separate optics. A reconsideration of that work in view of the JPL study results led to the adoption of a number of features of the JPL approach, including the Mills Cross geometry. The design for LASII discussed in this paper is the result of these previous studies plus a brief additional study at JPL.

2. Science

New discoveries in astronomy often result from significant increases in angular resolution. The images from the refurbished Hubble Space Telescope are revealing new objects and new structures that challenge our physical understanding. The post-COSTAR Faint Object Camera (FOC) on the 2.4 m H5T has reached diffraction limit at a wavelength of 486 nm,[6] namely 43 milliarcsec (mas). We have studied a small Laser Stabilized Imaging Interferometer (LASH) that will achieve a resolution of 7 mas in the visible, 6 times better than the FOC, and will aim for an even larger relative improvement to 2.5 mas at 150 nm. Many scientific problems can be addressed with LASII, and we expect significant advances in astrophysics to result from this substantial increase in resolution.

2.1 Background of the Imaging Interferometry Concept

For over a decade imaging interferometry has been frequently cited as the next logical step to achieve higher spatial resolution to succeed the accomplishments of HST. It is a challenging concept but one that lends itself to a midsize NASA mission. A number of ideas concerning optical imaging interferometry in space were presented at ESA and AAS workshops[7,8] in 1984. in 1986, the Ad Hoc Working Group on High-Resolution Imaging Interferometry in Space examined the various scientific opportunities for imaging interferometry in space, and recommended[9] the construction and flight of an "intermediate imaging inter ferometer." This was defined to

have an angular resolution "at least one order of magnitude greater" than that of HST. Further workshops were organized by ESA[10] in 1987 and NASA's Astrotech 21 program[3,11] in 1990.

In 1991, the report of the Interferometry Panel of the NRC Astronomy and Astrophysics Survey Committee ("the Bahcall Report") recognized that "despite the promise of interferometry carried out from the ground, the ultimate power of this technique will probably be fully realized only with a system operating in space, where no limits to the coherence size, angle, or time arc imposed by the terrestrial atmosphere."[12] Looking ahead to the new initiatives for the next decade, the Bahcall Report endorsed the action to "support planning and design of an advanced interferometer to be built in the next decade." In 1992 ESA sponsored a third workshop,[13] and the present conference series began in 1993. Ridgway[14] reviewed the scientific justification for a space interferometry mission in that latter meeting.

In view of the emphasis on "smaller, quicker, cheaper" missions, it is desirable and possible for LASII to obtain an angular resolution in the visible a factor 6 greater than presently achieved with the post-COSTAR FOC. The goal is a resolution of 2 mas at 120 run wavelength, 2.5 mas at 150 run wavelength, and 5 mas at 300 nm. The main emphasis will be on UV observations, although visible imaging will also be important. An IR imaging capability out to roughly 6 μ could be included if desired, although some compromise in the choice of mirror coatings would be needed. The magnitude limit for point sources is V = 2.5 in the visible (500 nm) and 24 in the UV (at 150 rim), based on a S/N of 5 in a total observing time of 2,000 s. In discussing the science which can be done with LASII, we will assume that three "looks" are obtained for each source, with the interferometer rotated by angles of 0, 30, and 64)* about its axis in order to improve the WV-plane coverage. The Fourier transforms of the images will be cleaned to reduce the noise and artifacts, and then optimally combined. The expected high quality of the image is shown in § 3.2. The various types of sources for which LASII observations would be particularly valuable are discussed below. Figure 1 shows the angular size of a number of these objects as a function of distance based on the S/N of 5 in a 2,000 s integration,
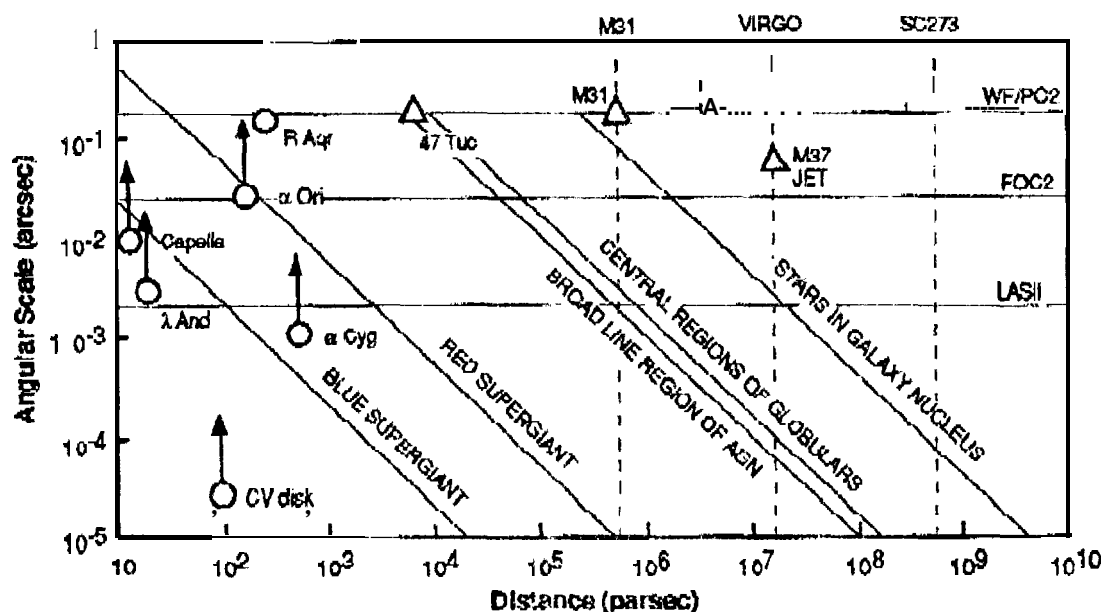

Figure 1. Apparent angular size of a variety of objects as a function of distance. The angular resolution of the WFPC2 (160 run),F(X2050 run), and LASII (150 nm) are marked by the horizontal lines. The positions Of jets, clusters, and galaxies as imaged in the ultraviolet are denoted by open triangles. A few candidates for imaging stellar surfaces, chromospheres and coronas in single stars and binaries are marked by open circles.

2.2 Advantages of Ultraviolet Imaging Interferometry

The scientific advantages of imaging astronomical targets in the ultraviolet (115 - 300 nm) region of the spectrum are many:

    * A wide range of plasma temperatures can be sampled, from ultraviolet transitions in CO or H II formed in the coolest material, to the highest temperatures of $2 - 3 \times 10^5$ K represented by strong resonance transitions of C IV and N V. Under collisional ionization equilibrium, the presence of an ion species *directly signals the electron* temperature in the plasma. Extremely varied physical conditions are accessible through ultraviolet measurements

    • Ultraviolet imaging eliminates (or greatly reduces) the confusion and background in the optical spectral region. Particularly outstanding examples noted later include the appearance of hot ultraviolet sources in crowded fields such as globular cluster cores and galaxies.

    • A great variety of targets, from planets and satellites in our solar system, to stars and stellar systems, to clusters and galaxies emit profusely in the ultraviolet spectral region, so that broad application of ultraviolet imaging exists across many subdisciplines of astronomy and astrophysics.

    • Exploration of the ultraviolet images and spectra from the post-COSTAR HST can aid in target selection.

The most important advantage of UV imaging, however, is the higher resolution which can be achieved for a *given aperture* size. If the use of laser metrology for active control of mirror displacements and tilts plus the minimization of disturbance sources is indeed able to achieve a quiet optical system at relatively low cost (see below), even in the UV, then the mission cost will be determined more by the size of the required structure than by any other factor. For sources which can be observed at any of a wide range of wavelengths, such as energetic jets, observations in the UV thus would be the most economical approach.

2.3 Extragalactic Objects

The imaging and resultant morphological classification of high redshift galaxies will be possible with LASII. The early results from the refurbished HST give evidence of mergers and interactions that affect the population of galaxies in clusters. However with diffraction limited resolution of 70 mas at 700 nm furnished by WFPC2, the first images point up the need for even higher resolution.[15] LASII will provide 8 mas resolution with 4?(oversampling. Imaging of galaxies in the ultraviolet will also reveal new components of the stellar population. An HST/FOC (pre-COSTAR) image of the center of M31, using a filter centered on 175 nm, showed more than 1 UV individual bright objects which are believed to be post-AGB stars. Some objects appear slightly extended, which could result from a surrounding planetary nebula. In the optical, post-COSTAR images of putative companions to a $z=2$ quasar revealed twice the number of faint objects found previously.[15]

.4 major target of LASII is the imaging of active galactic nuclei to examine the physical structure of the narrow line region. Typical sizes are 100 pc to 1 kpc, which for the closest Seyfert galaxies (NGC 41S1 and NGC 1068) give angular sizes of 1000 mas and are accessible to HST. One of the first refurbished HST/FOC images of the narrow line region of NGC 1068 shows an extremely complex structure containing bright filaments and patches intermingled with dark lanes.[16] LASII will rosily resolve more distant AGN sources. Narrow line regions in objects as distant as 100 Mpc should be resolved and imaged. Thus substantial information on the gas flow patterns around AGN's will be obtainable.

It is worth noting that the post-COSTAR FOC images of the nuclear region of the Seyfert galaxy NGC 1068 revealed 10 point sources where only one had been found in the pre-COSTAR image.~[6] We expect a greater increase in the number of sources detected with LASII images.

Observations with LASII are expected to extend the search for massive black hole relics in galactic nuclei from earlier quasar or AGN phases to larger distances. Recent observations in galaxies such as M31 and M87 give strong evidence for central massive black holes. The WFPC2 narrowband H_α and [N II] images give direct evidence for a small disk of ionized gas with apparent spiral structure surrounding the nucleus of M87. Ford at al[17] *have identified this structure* as a disk surrounding a black hole. A 10^8 M$_\odot$ hole should produce a roughly

15 pc luminosity cusp in the galactic center, imagable out to 200 Mpc. The cusp and surrounding stars have enough surface brightness to be detectable with 100 nm bandwidth. It may also be possible to determine some information on the velocity dispersion as a function of radius.

The physical connection between the broad line region and the material contained in the nonthermal jets is another puzzle of AGNs. LASII will be able to resolve the structure of the jets, and objects similar to the braided jets in sources such as NGC 4258. About 100 mas resolution at 220 run was achieved with the pre-COSTAR FOC on HST in an image of the jet emerging from the active galactic nucleus of M87. The filamentary patterns of the gas in the jet are revealed, as is the overall complex structure reminiscent of the 2 cm map made at the VLA.

High resolution imaging of a multiple component gravitational lens allows LASII to capitalize on the magnification of a lensed quasar. This extra 1-dimensional magnification is typically on the order of 50. Thus the effective resolution on the quasar itself is approximately $FWHM/(50 \times 4)$ where the 4 accounts for identification of features cm a scale less than the point spread function. When the FWHM equals 2.5 mas, the resolution at the quasar would be 12 μas. For a quasar at z=2.73, this corresponds to a spatial scale of 1.5×10^{17} cm which is about 10 times smaller than the broad line region in 3C273-like objects. Thus LASII should be able to resolve the broad line region of quasars. Gravitational lens systems to be observed would include the Cloverleaf (H1413+117), the Einstein Cross (Q2237+0305), and UM 673. An image of a lensed quasar in the core of a narrow line should show visible extent, and an image in the broader parts of the line has a good chance of showing visible extent. LASII could also search for millilensing systems with separation of 1 to 100 mas due to lensing by masses of $1 0^6$ to 10^9 M⊙. VLBI techniques are being applied at radio frequencies to search for such systems; LASII could extend this through the optical region.

2.4 Globular Clusters

Globular clusters make attractive targets for ultraviolet imaging. Star densities near their cores are higher by 10^4 as compared to the solar neighborhood; milliarcsecond resolution is required to separate stellar images at the distance of M31, for instance. The kinds of objects inhabiting clusters, and in particular the centri core reflect both stellar evolution and the dynamical evolution of the cluster. Ultraviolet imaging can contribute uniquely in defining the contents of globular clusters because ultraviolet emissions are sensitive to the hot stellar component (horizontal branch stars and white dwarfs) while eliminating contamination from the visible. Knowledge of the ultraviolet radiation field produced by the globular clusters is necessary to understand the ionization of our galactic halo, and may also relate to the puzzling ultraviolet upturn found in elliptical galaxies.

The dramatic difference between color magnitude diagrams in the visible and ultraviolet shows the domination of different types of stars in the two wavelength regions. Ultraviolet images of the globular cluster ω Centauri were obtained with the Ultraviolet Imaging Telescope (UIT) on the ASTRO mission. The spatial resolution of UIT corresponds to 3 arcsec. With the passband centered at 162 nm, and a solar-blind defector, the stellar content of evolved hot horizontal branch stars and early post-AGB stars is clearly visible. These images enabled additional ultraviolet-bright stars to be discovered. Much higher spatial resolution (point spread function of ~70 rnas FWHM for the F/96 mode and of 160 mas FWHM for the F/48 mode) was obtained with the HST/FOC (pre-COSTAR) that imaged the core of the rich globular cluster 47 Tucanae. A high density of blue straggler stars was discovered in support of the idea that these objects are formed by collisions and coalescence in the dense core of the cluster. Confirmation of the dynamical evolution of globular cluster stars represent-s a fundamental challenge both to the observations and our *theoretical* understanding. Hardly any of these blue stragglers were found in deep B and'? images, indicating V fainter than the threshold of 16.5. 'his result underscores another unique contribution of ultraviolet imaging. Ultraviolet images are showing an otherwise unobservable stellar component of globular clusters.

WFPC2 observations of globular clusters show the central region to be fully resolved in NGC 6681.[18] However analysis of the images of M30 requires accurate modeling of incompleteness as a function of stellar density to

derive reliable star counts near the center of the cluster.[19] In such dense cores, the high angular resolution of LASH will be required.

2.5 Stellar Physics

Obtaining images of stellar surfaces and winds with LASH would establish a new area of stellar physics research and address many fundamental questions about stellar structure and atmospheres.

For cool stars, we expect to find substantial structures, of varying scale, on the surfaces of other stars. Several techniques already hint at the presence of structures on the surface of troth single stars, and stars in binary systems. Optical surface image reconstruction has been achieved in rapidly rotating cool stars with the surprising result that spots frequently occur at the poles.[20] Images of stars with different effective temperatures and gravity can establish the presence and character of atmospheric features under extremes of physical conditions. We expect the contrast of these structures to be much higher in the UV spectral region than in the visible, because the photospheric continuum is weak or absent in the UV. It should be remembered that the UV emissions arise from the chromospheres, transition regions, and coronas of COOI stars. These regions lie above the stellar photosphere, and in giant and supergiant stars can extend 2 or 3 stellar radii, making an ultraviolet stellar image a larger target than at visible wavelengths.

Direct ultraviolet imaging with the Faint Object Camera on HST reveals a strong jet in the mission line of C III (190.9 nm) near R Aqr, a Mira variable which is a component of a symbiotic binary system. Because Mira is a very cool star, its ultraviolet continuum is missing or weak, and the emissions from the jet can be isolated easily. Apparently a continuous input of energy is required to maintain this jet, suggesting that the ionizing source has a power law distribution. The source of this energy is unidentified.

Disks around pre-main-sequence, optically visible T Tauri stars (the classical T Tauri stars) and the inner regions of jets associated with Herbig Haro objects also appear to be good candidate far imaging with LASH. For disks on the order of the size of the solar system (10^8 - 10^9 km), they could be easily imaged out to nearly one kpc. For a nearby system at 150 pc, angular resolution of 2.5 mas gives about 15 resolution elements across the disk. The jets will certainly be resolvable, but with rather low surface brightness. W imaging of such disks and jets can define the velocity fields in these objects, and identify the source of the outflow from these objects. There are current indications that the fast outflow is not arising from the poles of the stars themselves, but from the equatorial regions or the surface of the surrounding accretion disk. This material is collimated above the disk into a fast jet-like wind.

Lamers[21] has discussed the information which can be obtained by imaging hot stars in the UV and visible. Early type supergiants have extended stellar winds, with mass loss rates on the order of 10^{-7} to 10^{-6} M$_\odot$/yr and wind velocities of 200 to 3000 km/s. The W spectrum of these stars shows that the winds are "superionized": high ionization species such as O VI and N V are observed in the winds of stars with $T_{eff} \geq 30,000°$ K. Moreover, most of the hot stars are X-ray emitter%[22] Both features clearly indicate the presence of radiation driven shocks in the winds, which produce a mixture of hot shocked gas (T~3×10^8 K) and cool gas (T~3×10^4 K) in the winds of hot stars. The origin of these shocks and their spectral distribution is largely unknown.

Using LASH to image the winds of hot stars in selected UV lines will answer the following questions
- Where do the shocks originate and how fast do they grow?
- What is the filling factor of the hot gas and how is it distributed?
- Is the wind spherically symmetric or can rotation produce flattened winds? (the winds of Wolf-Rayet stars show polarization which indicates non-spherical winds).
- Are there rotation-dependent "structures" in the winds? (suggested by the variability of the discrete absorption coefficients).

Explosive events such as novae also are of interest. Three or more novae with magnitudes of 2 - 8 appear each year. These will be prime candidates for study with high resolution instruments because they are so bright and

they become more resolvable as they expand. Producing a crude 3-beam image as early as 10 days after the explosion, LASII could be used to study explosion asymmetry, detailed flow in the ejecta, the formation of dust, and abundance gradients with spectral resolutions much smaller than the 3 nm emission line widths.

Supernovae are much more distant and therefore not imagable until some 50 years after a typical event 10 Mpc away. [SN 1987A is, of course, a notable exception.] Light echoes of the maximum light burst expand 30 times faster, however, and are imagable as early as 1.5 year after the event, if the surface brightness and dynamic range are observable.

2.6 Planetary Astronomy

When LASII is used as a planetary camera, the resolution at 300 nm on the surface of various targets is as follows: Mars -2 km; asteroids -7 km; Jupiter -15 km; Saturn -30 km; Neptune* 100 km; and Pluto -125 km. Blurring due to planetary rotation of atmospheric motions is not a problem since the exposure times needed to reach 100:1 signal-to-noise ratio are shorter than the estimated blurring times. Long term monitoring of atmospheric flows, volcanism, etc., would be possible, in addition to images of Pluto and asteroids 20-40 resolution elements across. The Voyager resolution for Jupiter was about the same as that of LASII.

3. Instrument

The design of the LASII instrument is driven by three goals: a resolution at least 6 times that of HST, a collecting area about equal to FIST and a useful wavelength range from 115-700 nm. The instrument is an imaging interferometer with a partially filled, segmented primary aperture in which the segments are all conjugate with a common secondary mirror, and the beams are combined in the image plane. The 24 primary mirror segments are organized into 4 separate arms arranged in a Milk Cross geometry shown in Figure 2a. The maximum baseline of the instrument's aperture is 15 meters.

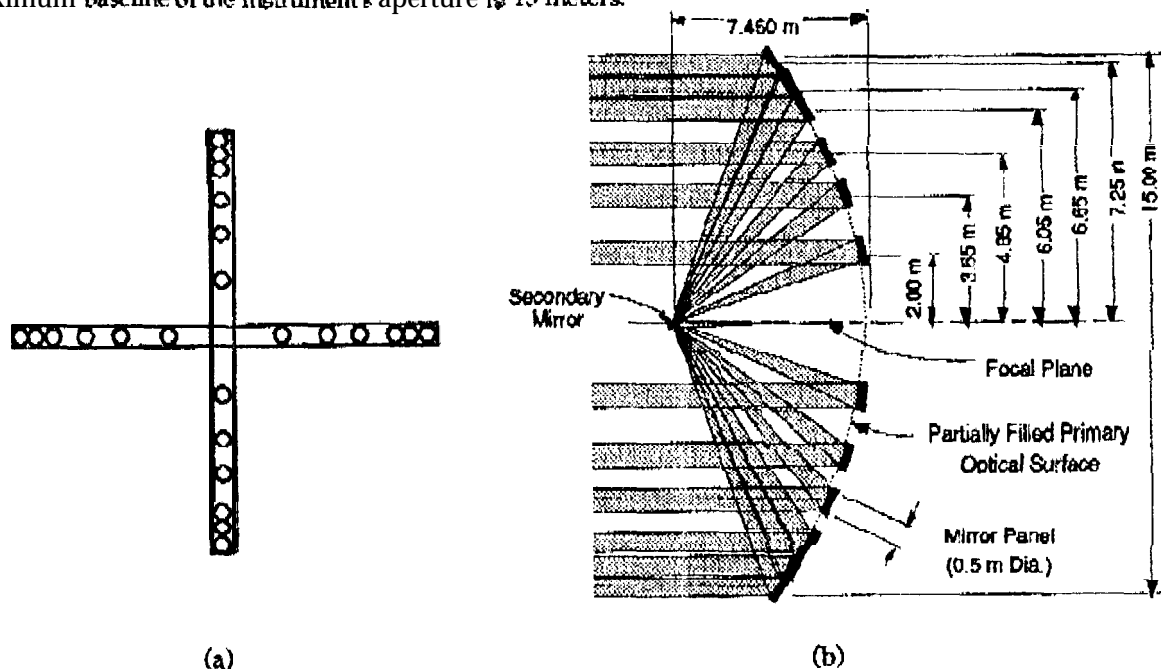(a)   (b)

Figure 2. Geometry of the LASII primary sub-apertures showing (a) arrangement of the 24 sub-apertures and (b) spacing and curvature of the primary mirror surface.

in order to operate effectively in the *W-to-visible* band, the optical pathlength differences from each of the sub-apertures must be controlled to the order of $\lambda/10$. Previous studies have suggested that maintaining alignment to such a tight tolerance without active control of the optics is very difficult indeed, as small temperature variations over the structure can induce dimensional change on the order of or larger than the imaging wavelength. Furthermore, a large optical structure hinds to have a low resonance frequency, and is therefore susceptible to structural disturbances excited by momentum wheels and other mechanical noise sources.

Recognizing the difficulties in maintaining tight structural tolerances, LASII will employ a laser metrology system to control the alignment of its sub-apertures. Optical path length differences between different mirror segments will be measured by an active laser metrology system to stabilize the optical path lengths during the integration period. Furthermore, vibration isolation and structural damping technologies will be applied to decouple the telescope *structure from the disturbance* inputs originating cm the spacecraft. Given the recent advances in active structure damping, vibration isolation, precision laser metrology, integrated modeling and stable, lightweight structural material technologies, we believe that the first mission to demonstrate interferometric imaging can fit within the scope of an Intermediate mission.

3.1 Main Telescope

The minimum LASII telescope design provides a 9.0 arcsec full field of view. The baseline optical design is a simple two-mirror Ritchey-Chretien telescope arrangement with a partially filled primary mirror aperture, in order to effectively deconvolve the images from the telescope point spread function (PSF), the central fringe of the telescope PSF should be greater than or equal to 3 pixels wide on the focal plane. For a 2048x2048 CCD with 9μm pixels, the resulting focal length requirement for LASII is 1,125 meters, or a f/75 design.

Because of the cost consideration imposed by the desire to fit within the scope of an intermediate-class mission, the LASII optical design is constrained by the launch configuration and must fit into a Atlas II fairing. This imposes a stringent demand on the primary-secondary spacing of the telescope, and leads to a fast primary mirror design. The proposed baseline configuration of the LASII optical system is shown in Figure 2b. The primary collecting aperture consists of twenty-four 0.5 meter sub-apertures arranged in a cross with each arm of the crow containing six sub-apertures to provide light collecting power comparable to that of the Hubble Space Telescope (HST). Each segment of the primary collecting surface is an off-axis section of a master parabola centered on the axis of the cross. The primary surface has a focal ratio of f/0.5, which resulted in a primary-secondary spacing of 7.46 meters. The secondary mirror is a short focal length hyperbola that is also centered on the axis of the cross. The spacing between the sub-apertures varies to provide good spatial frequency coverage, with those near the outside end of the arm being the closest together. A three mirror design was also briefly considered. This design performs well *over a* much larger field of view and is corrected for field curvature and coma. The possibility of using a three or four mirror design will be revisited in order to obtain a larger field of view.

The telescope, as designed, has an rms wavefront error of about 0.025 waves at 200 nm. In order to achieve diffraction-limited imaging, the optical path length difference between sub-apertures must be controlled to within a small fraction of the wavelength. To achieve a Strehl of 0.8, rms path length difference better than 9% of the wavelength (this is equal to 13 nm for 150 nm imaging wavelength) must be achieved. Additionally, the radius of curvature for each of the sub-apertures needs to be controlled to within 100 nm to achieve the desired optical performance.

The stringent demand on the manufacturing and control of the optical structure, although formidable, is achievable with only moderate technology development. Electron beam figuring has been used to figure the 1.5 meter panels for Keck with less than 40 nanometers of figure error (including radius of curvature). With only moderate development, this technology can be used to figure the primary *mirror* sub-apertures.

conductivity for solar energy from the surface down to the main structure. The solar radiation input can be further controlled by an observation strategy which minimizes changes of the solar radiation angle of incidence. Additionally, a sun shade can be deployed to prevent direct sunlight from hitting the secondary mast. This not only eliminates the problem of differential thermal expansion due to shadows cast by the primary arms, but also keeps stray sunlight out of the optics.
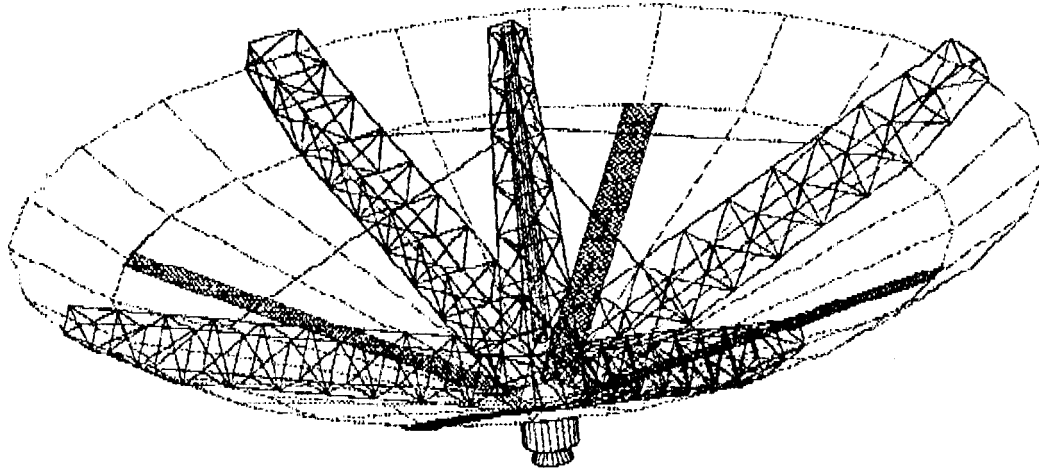
Figure 4. Deployed configuration of the LASII structure. The four trusses forming the Mills Cross, the tipeed mast supporting the secondary and laser metrology blocks and the spacecraft bus are shown with solid lines. The sun shade is shown with dotted lines. The hatched areas are solar arrays on the backside of the sun shade.

Other sources of quasi-static deformation include gravity gradients, aerodynamic drag and photon pressure on the structure. The effect of these sources has not yet been analyzed in detail, but it is expected that the magnitude of the distortion will be small compared to thermally induced distortions.

3.4 Focal Plane Instrumentation

Most of our study effort to date has concentrated on the design of the main telescope and the mission concept. However, an instrument with LASII's resolution, collecting area and spectral coverage will need a competent set of focal plane instrument. We anticipate that this will include a filter wheel-camera instrument and a W/visible spectrograph. These instruments could be mounted on an instrument turret whose axis of rotation is parallel to, but offset from, the optical axis of the telescope. An IR camera and an IR spectrograph would need to be included if the interferometer wavelength range is extended.

The filter wheel and camera would perform imaging observations. An array of interference filters, covering wavelength bands from 115 nm to the visible, would be mounted in a wheel for selection. Depend@ on the sensitivity of detectors available at the technology cutoff date, one or more areal arrays would capture the filtered images. We would expect to be using 2048x2048 arrays, or larger, to span the 3.0 arc sec, or larger, field.

The main spectrograph would consist of a common prefilter wheel, slit, shutter and rotating grating, and as many detectors as necessary to span the far UV to the visible. Again, the detector complement would include the most appropriate array sensors available, whether they be CCDs, enhanced CCDs or some other type of device.

3.5 Control and Guidance System

The LASII instrument will require separate guidance and optical control subsystems to provide fine guidance and optical path length stabilization during observing.

Image degradation can result from either the rigid body motion of the spacecraft or the dynamic deformation of the instrument. Over the expected integration time, the drift of the image on the focal plane should be less than 10% of the diffraction-limited point spread. For LASII, this translates to a 3 nrad pointing stability requirement over the 1,000 to 10,000 s integration time. This precision pointing control is achieved with a set of guide star tracking telescopes and a reaction wheel assembly. Furthermore, in order to obtain near diffraction-limited images, individual mirrors must be phased to maintain the optical path length difference to $\lambda/10$. For LASII, this stringent demand on the instrument control is met by a combination of active structure isolation and precision laser metrology.

3.5.1 Structural Deformation Control

Compared to the structural distortion generated by thermal changes or mechanical creep, the distortion generated by dynamic disturbances is typically of higher frequency. The principal sources of dynamic diaturb.ante, when thrusters are not in tree, are the reaction wheels. The actual disturbance spectrum consists of a broadband base spectrum and a series of narrowband spikes, the frequencies of which are at the primary structural resonance frequencies. Previous studies of large spaceborne optical interferometers such as OSI and POINTS indicated that uncompensated reaction wheel motion will impart micron-level disturbance spikes when multiples of the wheel speed agreed with structural resonances. The HST reaction wheels operating at their normal speeds were assumed. In order to obtain near-diffraction-limited images, disturbances must be reduced to about a tenth of the Wavelength.

The above requirement will be met for LASII by a combination of three approaches. In an earlier imaging interferometer study at JPL,[26] the reaction wheels were assumed to run at low rates and the resulting structural vibrations were considerably lower. If LASII is flown in a 900 km circular orbit, gravity gradient torques which lead to cumulative spin-up of the wheels can be minimized by making the moments of inertia perpendicular to the optical axis nearly the same, and by equalizing the times spent in the three different azimuth orientations. Secondly, Field Emission Electric Propulsion (FEEP) thrusters, which are being developed by ESA, would be used to control the interferometer orientation during observations, so that the wheel speeds can be kept away from resonances. Such thrusters have htgh specific impulse at low thrust, and are expected to have long lifetimes.

The third approach for LASII would employ vibration isolation techniques to control the vibration induced by the reaction wheel assemblies, or by any other on-board disturbance sources. A number of isolator designs were considered, and a combined active/passive soft mount was baselined for the isolator design. The combined active/passive soft mount allows for improved isolation performance compared to a purely passive soft mount. The mount consists of a passive soft mount and an active actuator which is slaved to a force sensor mounted near the quiet destination. The passive soft mount can be developed with a corner frequency as high as 20 Hz to provide the stiffness necessary to limit the amount of travel and to (possibly) eliminate the need for a complex latch mechanism during launch. Active feedback based on the force sensor output is then used to reduce the effective force load on the quiet structure. An effective isolator corner frequency as low as 0.2 Hz can be achieved with active feedback. The isolation stage provides, in effect, a low pass filtering of the momentum wheel disturbance, and a lower corner frequency permits a more effective damping of higher frequency disturbances.

For optical system distortions at lower frequencies, such as those generated by changing thermal gradients, the metrology system measures the tip, tilt and three translation modes of each mirror segment. This is accomplished using two metrology control blocks located on the secondary boom. The locations of the control blocks are illustrated in Figure 5. Four retroreflectors mounted on each mirror segment permit measurements of tip, tilt and displacement motions from each control block with some redundancy. The metrology launcher located near the secondary mirror can be thought of as measuring the distances between individual mirror segments and the secondary mirror. A second control block located orr the secondary boom near the primary mirror measures essentially the radial distance changes. Measurement between the control blocks and the secondary are also required. Metrology beams from launchers located on the secondary mast are insensitive to

rotation around the telescope axis. Fortunately, the performance of the telescope is insensitive to this rotational motion, and therefore the non-observed mode has little impact on the controllable modes.
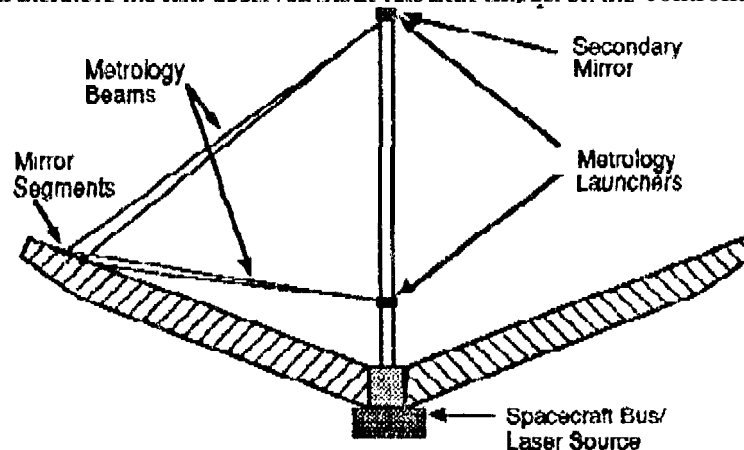

Figure 5. Location of the metrology launchers

In general, each metrology beam launcher (optical head) measures the displacement of the target retroreflector relative to a reference retroreflector. To tie all of the metrology gauges to a common reference, the beam launchers will be mounted on a common, dimensionally stable block. Ninety-six beams from each block will be required to provide metrology to the 24 science apertures located on the arms of the telescope. Additionally, a number of metrology beams will be required to stabilize the position of the guide telescopes.

A flight qualified implementation of the metrology system will be made possible by advances in frequency stabilized lasers, fiber optics, modulators and integrated optics technologies. The use of fiber optic components simplifies alignment and increases reliability. Polarization maintaining fibers and star couplers can be used to distribute the laser light from a single source to multiple launchers. Recent advances in moderate power (300 mW) single-longitudinal-mode Nd:YAG lasers have made it possible to feed a large number of the metrology beams from a single laser. This eliminates the need to frequency-lock multiple metrology lasers and hence considerably simplifies the system design. Different modulation frequencies can be used for different beams to avoid moss-talk. The laser frequency stability requirement to achieve nanometer-level measurement accuracy over a path length of 7 m is approximately 30 kHz. However, a given fractional change in all of the optical metrology paths would not distort the optical system to first order. An external cavity will be used to stabilize the laser to the desired **frequency** stability.

3.5.2 *Telescope* Pointing *Stabilization*

The LASII telescope pointing must be stable to within a few nanoradians such that image blurring resulting from pointing is small compared to the width of the point spread. The required absolute pointing accuracy, on the other hand, is considerably less stringent as we only need to position the object within the field of view of the science aperture. An absolute pointing accuracy of 500-1000 nrad is adequate for a science field of 3.0 arcsec.

Because of the long focal length of the imaging optics and the offset angles of 5 or 10° needed to locate guide stars of sufficient brightness, it is not feasible to use the main apertures for guide star tracking. Instead, separate guide interferometers or telescopes are used to provide fine guiding for LASII during imaging. Several concepts for guide star tracking have been evaluated, including the use of two white light interferometers with three apertures each to accurately control the main interferometer orientation- Delay lines in the guide interferometers would not need to move during observations. Another guiding concept employs two separate telescopes mounted on the arms of the interferometer. These guide telescopes would be of simple Cassegrain design with 0.5 meter aperture- Either type of guiding system can be designed with 1-2 mas guiding knowledge.

One critical aspect of the guide star tracking concept is the relative alignment between the science apertures and the guiding system. This relative alignment will be measured and controlled using the same laser metrology system used to maintain active alignment between individual sub-apertures.

4. Launch Vehicle, Deployment and Operations

The LASII spacecraft is designed around three major components, the science payload, the bus and the launch vehicle adapter. The engineering subsystems are supported by a bus structure located at the lower end of the optical telescope. It is less than 1 m high and has a total outside diameter of no more than 2 meters. The spacecraft/launch vehicle adapter supports the spacecraft on the Atlas II launch vehicle. The mass of the spacecraft is estimated to be approximately 2300 kg, including approximately 1300 kg for the mass of the optical telescope.

4.1 Launch vehicle

An Atlas 11 is baselined for the LASII launch. The choice of the launch vehicle is dictated by the dimension of the launch fairing, lift rapacity, and cost. A larger launch vehicle such as a Titan IV has large enough fairing and lift capacity, but would cost too much. On the other hand, smaller launch vehicles such as Delta II and Titan II have fairings that are too small and lack the lift capacity to reach a sun synchronous, or higher, orbit.

The Atlas launch vehicle can have a large launch fairing (13.75 ft outer diameter and 40.1 ft length). A dynamic envelope of 9.5 meter long and 3.6 meters wide is sufficient for the proposed LASII launch configuration shown in Figure 6. The four arms of the interferometer, the solar army panels, and the sun shade are folded against the secondary mast and secured during launch. Atlas II also provides more than adequate lift capacity, approximately 4300 kg to a 900 km sun-synchronous orbit (with approximately a 1500 kg margin), and probably adequate lift capacity for a high Earth orbit or for solar orbit,
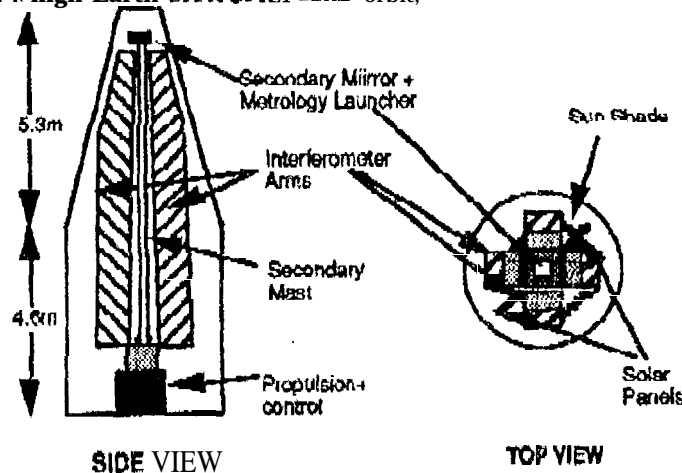

Figure 6. LASII launch configuration.

4.2 Deployment Concept

Upon reaching the desired orbit, the deployment sequence for LASII is very straightforward. First, the launch shroud and the retainer ring will be jettisoned. Spring loaded braces will then unfold and lock into place. Worm drive actuators can be used to assist joint straightening if necessary. Using actuators, the knee joints are expanded along the axis to preload truss arms and put braces under *mmqx-mien*. Long term loading of the braces could be maintained by the worm drive actuators.

The solar panels will be deployed using a similar concept. They are rotated 90 degrees in a stowed configuration, as is shown in Figure 5. The panels will be rotated after unfurling and locked into the deployed position. The sun shade is attached to both the interferometer arms and the solar prowls and folded accordion style. It will simply extend during the ~~~~~~~ ~~~~~. The deployment of LASII is shown in Figure 7.

Spring Loaded Braces

Lock-knee joint with worm drive actuator

(a)   (b)   (c)
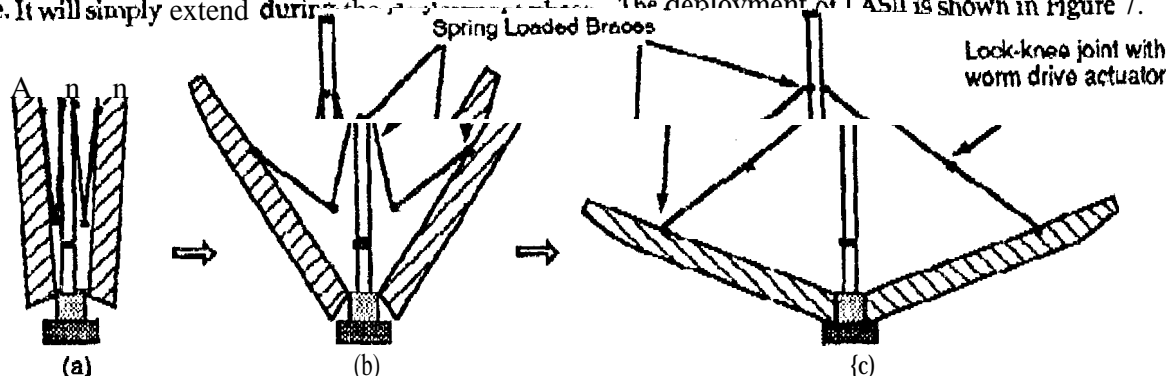
Figure 7. Deployment sequence of LASII: (a) Jettison launch shroud and retainer ring, (b) unfold spring loaded brace joints, and (c) lock knee joints straight and preload the truss arms with worm drive actuators to main compression pressure.

4.3 Operational Procedures

4.3.1 Initial alignment

After deployment and on-orbit check out, the spacecraft will undergo an initial alignment phase. The purpose of this phase is to achieve relative phasing for individual sub-aperture mirrors and to calibrate the laser metrology system for possible offset errors introduced during launch. During this phase the segments of the primary mirror will be phased relative to each other using the following steps:

1. First, the telescope will be slewed to position a bright, unresolved guide star within the science field of view.

2. The segments are then co-aligned by adjusting them in a spiral pattern, one-by-one, until the signal is co-aligned. The proper actuator commands are remembered so that they can be tilted away to remove the light from the detector and later tilted back.

3. With all the segments but one tilted away, and that one aligned, the piston mode for that segment is adjusted to maximize the signal intensity (focus adjustment).

4. Using one of the segments as a reference, the segments are then pair-wise aligned and phased until the best alignment is achieved.

5. The last and final stage of alignment will be conducted using focal plane sharpening algorithms. A simulated annealing algorithm has been successfully applied to sharpen images, and the error in the conic constant of the Hubble Space Telescope was successfully estimated using this approach.

6. Once initial co-phasing is reached using guide stars, the relative position of the segments will be measured by the laser metrology system. The measured distances will then be used to correct for subsequent motions.

4.3.2 h4uhwz.ante alignment

Maintenance realignment will be conducted periodically to ensure proper phasing of the target. It is envisioned that the telescope will undergo realignment by observation of bright stellar objects as necessary.

This corrects for slow drift of the laser metrology system due to effects such as thermal changes in the primary mirror apertures, the secondary and the control blocks.

4.3.3 Observing

During the operation, the telescope will observe within at least a 45 degree cone from the anti-sun point. The cone angle can be increased in order to obtain more complete sky coverage by adding an additional sun shield in one quadrant of the interferometer. It is anticipated that three separate looks at targets separated by 30 degree rotation around the telescope axis will be taken. With integration periods of 1,000 to 10,000 c per look, this will permit imaging of objects dimmer than 25th magnitude. The observation data will be stored onboard the solid state recorder as part of the Command and Data Subsystem. The data will then be downlinked using the 26 meter net of the Deep Space Network.

.5. ACKNOWLEDGMENTS

We would like to thank Steve Synnott, Rick Helms, Hamid Hemmati, Serge Dubovitsky, Bob Freeland and Dave Redding for their important contributions to this project.

6. REFERENCES

1. M. M. Colavita 1992, in *ESA Colloquium on Targets for Space-Based Interferometry*, (ESA SP-354), pp 177-.

2. S.P. Synnott 1991, in *Workshop Proceedings: Technologies for Optical Interferometry in spree*, (JPL D-8541, vol. 1), pp 31-41.

3. NASA 1991a, *Workshop Proceedings: Science Objectives and Architectures for Optical In terferometry in Space*, (JPL D-8540, Vol. 1), May 15,1991.

4. R.T. Stebbins, P.L. Bender and J.E. Faller 1987, in *Optical Interferometry in Space*, (ESA SP-273) pp 85-91.

5. P.L. Bender and R.T. Stebbins 1991, in *Workshop Proceedings: Science Objectives and Architectures for Optical Interferometry in Space*, (JPL D-8540), pp 101-105.

6. R. L Jedrzejewski, G. Hartig, P. Jakobsen, J.H. Crocker and H C. Ford 1994. *Astrophys. J.* 43S, L7.

7. ESA 1985, ESA *Colloquium on Kilometric Optical Arrays in Space*, (ESA SP-226), April, 1985.

8. A AS 1984, Workshop on High Angular Resolution Optical Interferometry from Space, *Bull. Amer. Astron. Soc.* 16,1%3 (Part II), pp 747-fK~7-

9. G. Field 1986, Letter Report of the ad hoc Working Group on High-Resolution Imaging Interferometry in Space, (to G. Newton, NASA HQ), 25 Nov. '86.

10. ESA 1987, *ESA Workshop on Optical Interferometry in Spree*, (ESA SP-273), 1987.

11. NASA 1991b, *Workshop Proceedings: Technologies for Optical Interferometry in Space*, (JPL D-8521, Vol. 1), Sept. 15,1991.

12. NAS/NRC 1991, Working *Papers for Astronomy and Astrophysics Panel Reports*, (Nat. Acad. Press, Wash., D.C.), pp V-1 to V-21.

13. ESA 1992, *ESA Colloquium on Targets for Space-Based Interferometry*, (ESA-SP-354), Dec., 1992.

14. S.T. Ridgway '1993, in SPIE 1947, *Spaceborne Interferometry* (SPIE, Bellingham, WA), pp 2-11.

15. A. Dressler, A. Oemler, W. B. Sparks and R. A. Lucas 1994., *Astrophys. J.* 435, L23.

16. F. Macchetto, A. Capetti, W. B. Sparks, D. J. Axon and A. Boksenberg 1994, *Astrophys. J.* 435, L15.

17. H. C. Ford, R. J. Harms, Z. I. Tsvetanov, G. F. Hartig, L. L. Dressel, G. A. Kriss, R. C. Bohlin, A. F. Davidsen, B. Margon, and A. K. Kochhar 1994, *Astrophys. J.* 435, L27.

18. A. M. Watson, J. R. Mould, J. S. Gallagher III, G. E. Ballester, C. J. Burrows, S. Casertano, I. T. Clarke. D. Crikps, R, E. Griffiths, J. J. Hester, J. G. Hoessel, J. A. Holtzman, P. A. Scowen, K. R. Stapelfeldt, J. T. Trauger, and J. A. Westphal 1994, *Astrophys. J.* 435, L55.

19. B. Yanny, F. Guhathakurta, D. P., Schneider, and J. N. Bahcall 1994, *Astrophys* 1., 433, L59.

20. S. Vogt and A. P. Hatzes 1991, in *Lecture Notes in Physics*, No. 380, 297.

21. H J. C. L. M. Lamers 1992, in *Targets for Space-Based Interferometry*, (ESA SP-354), Dec., 1992; pp 15%162.

22. J.P. Cassinelli and H.J.G.L.M. Lamers 1987, in *Exploring the Universe with IUE* (Kondo et al, eds.).

23. D.L. Meier 1991, in *Workshop Proceedings: Technologies for Optical Interferometry in Space,* (JPL D-8541, vol. 1), Sept. 15, 1991; pp 153-160.

24. M. San Martin 1991, in *Workshop Proceedings: Technologies for Optical Interferometry in Space,* (JPL D-8541, Vol. 1), pp 63-77.